CORPUS PUBLISHERS

Journal of Mineral and Material Science (JMMS)

ISSN: 2833-3616

Volume 5 Issue 1, 2024

Article Information

Received date : January 17, 2024

Published date: February 12, 2024

*Corresponding author

N Rulyov, Institute of Biocolloid Chemistry, National Academy of Sciences of Ukraine, Head of the Department of Physico-Chemical Hydrodynamic of Ultra-disperse Systems 42 Vernadsky av, 03142 Kyiv, Ukraine

DOI: 10.54026/JMMS/1079

Key Words

Minerals; Fine and Ultrafine Particles; Nano-Bubbles; Flotation; Aggregation

Short Report

Limitations of the Nano-Bubbles Application for Beneficiation of Fine and Ultrafine Particle Flotation

N N Rulyov*

Institute of Biocolloid Chemistry, National Academy of Sciences of Ukraine, Head of the Department of Physico-Chemical Hydrodynamic of Ultra-disperse Systems 42 Vernadsky av, 03142 Kyiv, Ukraine

Abstract

The flotation of small particles is one of the considerable global challenges facing the mineral raw materials processing industry today. In the recent 10 years, the effects of cavitation Nanobubbles (NB) on the efficiency of selective flotation of fine and ultrafine mineral particles have been explored in several experimental studies. Since the findings obtained in these studies are inconsistent and contradictory, there has been a need for a theoretical assessment of the potential of the above approach for practical applications in the area of poor fine-disseminated ores beneficiation. Application of the kinetic laws, describing the behavior of dispersed systems in a turbulent flow, has allowed establishing that, similar to flocculants, NB could bind hydrophobic particles into large aggregates and thus increase the efficiency of their capture by conventional coarse bubbles in flotation. It has been demonstrated that the optimal volumetric dose of NB per unit mass of particles could be calculated by the formula $f = 2d_b/d_p\rho_p$, where d_b is NB size, and d_p and ρ_p – respectively are the size and density of particles. Based on the real data, the optimal numerical concentration of NB was calculated, and the established value was found to be in the range (10^8-10^9) mL/L. The essential factor that limits practical applications of NB resides both in the low productivity of the known methods of NB generation and in the engineering difficulties of producing NB in sufficient quantities directly in the pulp. The last, but not the least important limiting factor is that the low concentration of small particles of valuable mineral in real pulps leads to very slow growth of such aggregates since the turbulence level in the flotation machines is almost by two orders of magnitude lower than the level required.

Introduction

Fine particles pose big challenges. The reason for that is obvious - the finer the particles are, the bigger the share of non-ferrous and rare metals lost into the mineral flotation tailings. This can be attributed to the effectiveness of the particle capture by a rising bubble, which, to a first approximation, is proportional to the square of the ratio of their sizes [1-6]. Thus, when the particle size decreases twofold, their floatability accordingly decreases fourfold, resulting in even higher growth of mineral beneficiation costs. For over 100 years, much effort has been invested in studies and tests for various ways to solve this problem [7]; however, so far, a universal solution has not been put forward. For example, one of the methods proposed involves increasing the particle size by aggregating them through the use of selective flocculants [8-11]. The second method has suggested to place small particles on larger carrier particles [11-15]. Another proposed approach involves the application of bubbles that have a size that is comparable to or not significantly larger than the size of the particles [16,17]. And though this method is being practiced in industrial water purification [18,19], it is not actually suitable for mineral raw materials beneficiation applications as the rising velocity of bubbles smaller than 100 μm is very low, and their generation in large amounts faces a number of engineering hurdles.

It has long been noted [20] that even small amounts of fine bubbles used in combination with conventional coarse bubbles lead to significant improvements in the flotation process. A theoretical justification for this phenomenon was given in [21], and the method of applying small bubbles in combination with coarse ones has been termed combined microflotation. The essential feature of this method is that small bubbles not only act as carriers for small particles, but besides, as it has been demonstrated in [22], assisted by these particles, they can combine into aggregates that can be effectively floated by coarse bubbles. Thus, hydrophobic particles serve as a connection link both between small bubbles and between their aggregates and coarse bubbles. The paper [22] provides the assessment of the optimal volume dose of small bubbles per unit mass of floated particles, which is determined by the formula

$$f = \frac{d_b}{2d_p\rho_p} \qquad (1)$$

where d_b is the size of small bubbles, and d_p and ρ_p respectively present the size and the density of particles. In the recent 10 years, the idea of applying nanobubbles for the purpose of promoting the flotation process of fine and ultrafine particles (below 10 μm in size) [23-29] has aroused substantial scientific interest since nanobubbles, as flocculants are able to bind such particles into aggregates and thus increase their floatability by coarse bubbles. The purpose of this study is to evaluate whether such combined nano-flotation has viable perspectives in terms of practical applications.

Nano-Bubble Generation

The best-known conventional way for producing Nanobubbles (NB) generation is based on the cavitation effect, where bubbles are generated from gas dissolved in water in a low-pressure zone. The easiest and most accessible method involves passing the air dispersion in a surfactant water solution through a device similar to a Venturi tube [30,31]. At the inlet to the tube, increased pressure is created, and thus, part of the air dissolves in water and releases in the form of nano- and micro-bubbles (MB) at the outlet of the tube into the normal pressure zone. Another option is to preliminary dissolve the air in a surfactant solution at high pressure and then release the solution thus obtained through a narrow tube into a medium with normal pressure [26]. In this case, besides NB, a considerable amount of MB will also be produced. We have used the data presented in [32] to produce the illustrative example shown in Figure 1 of the approximate frequency distribution of bubbles by size, which demonstrates that NB concentrate in the size range of 0.05 - 0.5 μm, MB concentrate in the range of 10 -1000 μm, whereas in the range of 1-10 μm there are practically no bubbles. This fact suggests that it is possible to separate NB from MB by the sedimentation of the latter, as was done in [31,33]. Recent theoretical studies [34-36] have shown that the existence of stable

NBs and their absence in the region of 1-10 μm can be attributed to the ratio of opposing capillary and electrostatic forces. In accordance with the Young-Laplace equation, the pressure that surface tension exerts on the gas inside the bubble is determined by the relation

$$P_{YL} = -\frac{2\gamma}{R_b} \quad (2)$$

where R_b is the bubble radius and γ is its surface tension. It can be easily calculated that the pressure created by capillary forces inside a bubble of 50 nm radius shall be around 30 bar, and, according to Henry's law, this should lead to dissolving the air present inside the bubble in water in microseconds. However, recently, it has been shown [37] that the bubble surface, even in distilled water, is always negatively charged due to the adsorption of OH^- and HCO_3^- ions. The presence of this charge produces the pressure due to the electrostatic repulsion of similar charges, and this pressure will be directed outward of the bubble. The value of this pressure can be estimated by the formula

$$P_E = \frac{Q_S^2}{8\pi\varepsilon R_b^4} = \frac{2\pi\sigma^2}{\varepsilon} \quad (3)$$

where Q_s is the total surface charge, ε is dielectric permutability of the medium and, $\sigma = Q_s / 4\pi R_b^2$ - is the surface charge density. Combining equations (2) and (3), we obtain the backpressure equilibrium condition in the form

$$\frac{P_{YL}}{P_E} = \frac{\gamma\varepsilon}{\pi\sigma^2 R_b} = 1 \quad (4)$$

Equation (4) suggests that sufficiently small bubbles with a high charge density and low surface tension may have a chance at least not being instantly dissolved.

It seems, it could be incorrect to assume that bubbles of 1-10 microns in size are not forming in the cavitation process. As it is known, cavitation bubbles tend to collapse producing a cumulative jet capable of destroying metal objects. It is possible that bubbles of the indicated size range are so short-lived that they are almost impossible to be registered, although there are publications showing the acts of their collapse filmed by high-speed photography (Figure 1).

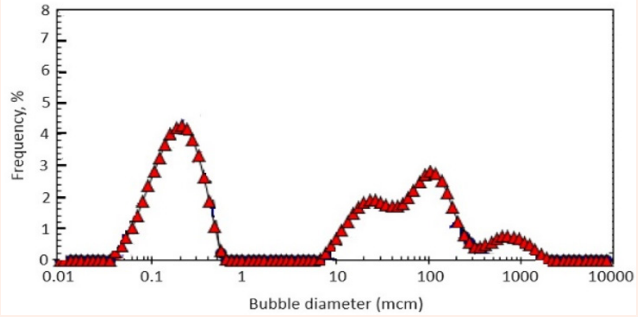

Figure 1: Frequency distribution of cavitation bubbles produced in Venturi tube. On the data from [32].

Optimal NB Dose

The optimal NB dose is defined as the volume NB dose per unit mass of particles that ensures their most effective aggregation as well as the aggregates' flotation by coarse bubbles. Since NBs do not aggregate with each other or with coarse bubbles, the excessive dose can block both the process of particle aggregation and their flotation by coarse bubbles. But when the NB dose is very low, the probability of particle aggregation at collision will be very low, too. Copying the pattern of flocculant use [38] brings us to the conclusion that the optimal dose of MB must correspond to a situation when nanobubbles should cover half of the particle surface. Let's assume that the numerical concentration of NB in the pulp is n_b, and that of floated particles is n_p. Then the volume dose of NB per unit mass of particles can be expressed by the formula

$$f = \frac{n_b d_b^3}{n_p d_p^3 \rho_p} = \frac{d_b}{d_p \rho_p} \frac{n_b d_b^2}{n_p d_p^2} = \frac{d_b}{d_p \rho_p} \frac{4S_b}{S_p} \quad (5)$$

where ρ_p is the density of particles, $S_p = n_p \pi d_p^2$ is the total surface area of particles per unit volume of pulp; $S_b = n_b \pi d_b^2 / 4$ is the surface area of particles that could be occupied by NB. Assuming in (5) $S_p / S_b = 2$, then we obtain for the optimal dose NB

$$f_{opt} = \frac{2d_p}{d_p \rho_p} \quad (6)$$

The formula (6) shows that the optimal NB dose increases with the decrease of particles size and density. For example, for quartz the optimal NB dose will be 4 times higher than that for chalcocite particles of the similar size. Applying equation (6) it can be easily shown that NB optimal NB volumetric concentration can be estimated by the formula

$$\varphi_{b\,opt} = c_p f_{nb\,opt} = c_p \frac{2d_b}{d_p \rho_p} \quad (7)$$

where c_p – is the mass concentration of floated particles. Thus, the optimal numerical NB concentration shall amount to

$$n_{b\,opt} = \frac{\varphi_{b\,opt}}{V_b} = \frac{12 c_p}{\pi d_b^2 d_p \rho_p} \quad (8)$$

Where V_b is volume of the single NB. For illustrative purposes Figure 2 shows the dependences of $n_{b\,opt}$ on the particle concentration c_p for various particle densities ρ_p, and these dependencies clearly suggest that the optimal NB numerical concentration lies in the range (10^8 - 10^9) mL^{-1}, and the optimal volumetric dose f_{opt} = (5×10^{-3} - 5×10^{-2}) mL/g of particles. Unfortunately, according to [31], this NB concentration could be achieved only if the dispersion would be passed through a Venturi tube for more than 20 times. Hence, more promising looks the method that involves the preliminary saturation of water with air at high pressure and the following throttling through a narrow channel [27]. Both alternatives would encounter engineering problems when applied in practice, since if the NB dispersion should be prepared in a surfactant solution and then fed into the pulp, this could result either in a strong dilution of the pulp, or could be accompanied by a strong decrease of the concentration of NB; or both cases may occur.

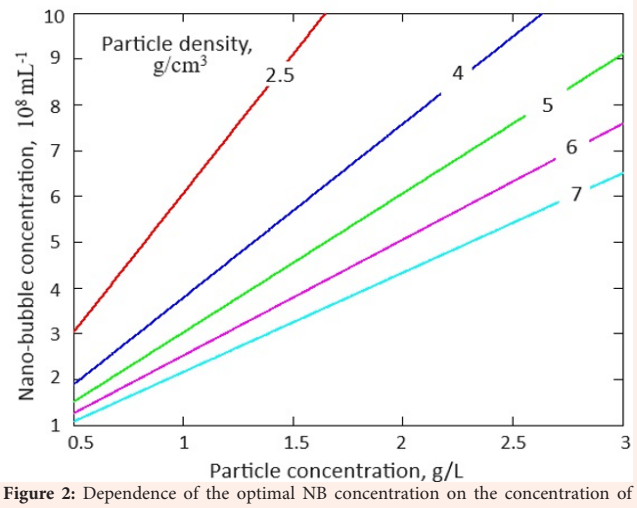

Figure 2: Dependence of the optimal NB concentration on the concentration of floated particles and their density: d_b= 0.5 μm; d_p = 10 μm.

Aggregation Rate of the Particles

Figure 3 illustrates that the process of forming aggregates of floated particles comprises three stages: 1- mixing particles with an optimal dose of NB; 2 - deposition of NB on the surface of hydrophobic particles and 3 - formation of particle aggregates with the aid of forming NB bridges between them.

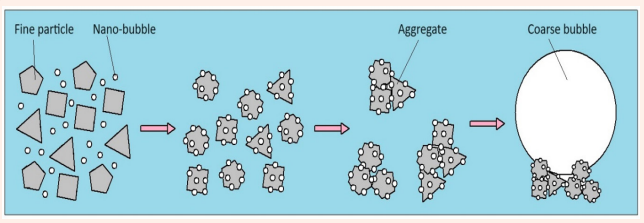

Figure 3: Stages of the combined nano-flotation of fine particles.

Since the sedimentation of both NB and fine particles proceeds very slowly, the deposition of NB onto the particle surface will occur mainly due to the inhomogeneity of the hydrodynamic field in the flotation cell. In this case, the rate constant of the process can be estimated by the formula [39]

$$K_{bp} = \frac{4G\varphi_p}{3\pi}\varepsilon\left(d_b/d_p\right) \quad (9)$$

where G is the medium average shear rate, φ_p is the volume concentration of particles in the pulp, $\varepsilon(d_b/d_p)$ is the probability of NB attachment on the surface of a particle at their collision in a simple shear field. The results obtained in [40] show that in case when $d_b \ll d_p$, the function $\varepsilon(d_b/d_p)$ takes the form

$$\varepsilon = \frac{d_b^2}{d_p^2}\alpha \quad (10)$$

where α is a parameter that depends on the nature of the surface forces of interaction between the particle and the NB. Thus, as it is demonstrated by formulas (9) and (10) the rate constant of NB deposition on the surface of particles can be obtained as

$$K_{bp} = \frac{4G\varphi_p d_b^2}{3\pi d_p^2}\alpha = \frac{4Gc_p d_b^2}{3\pi\rho_p d_p^2}\alpha \quad (11)$$

According to the Smoluchowski equation, modified with the account of the aggregate's porosity [41], that in this form describes the process of the aggregate growth on a simple shear hydrodynamic field, we arrive at

$$\frac{d\left[d_A(t)\right]}{dt} = \frac{4G\varphi_p\lambda}{3\pi(1-p)}d_A(t) \quad (12)$$

where d_A presents the aggregate size, p is their porosity, λ is the probability of particle aggregation upon their collision in a simple shear field due to the formation of NB bridges, depending on the ratio of surface and hydrodynamic forces. Thus, the rate constant of the second stage can be estimated by the formula

$$K_{pp} = \frac{4G\varphi_p}{3\pi(1-p)} = \frac{4Gc_p}{3\pi(1-p)\rho_p}\lambda \quad (13)$$

Considering that α and λ parameters are smaller than unity, and next assuming these parameters equal to unity, it is possible to estimate the maximum value of the total rate at second and third stages of particle aggregation that shall be determined by the smaller of the two rate constants K_{bp} and K_{pp}. Since the constant K_{bp} differs from the constant K_{pp} by the factor $d_b^2/d_p^2 \ll 1$, then this very constant will determine the rate of particle aggregates growth. Figure 4 shows the dependence of $K_{pp\ max}$ on the particles concentration and density; and this dependence proves that at shear rate common for flotation cells, the process goes very slowly. It will take at least 100 minutes to enlarge the aggregates to the sizes of about 70 microns.

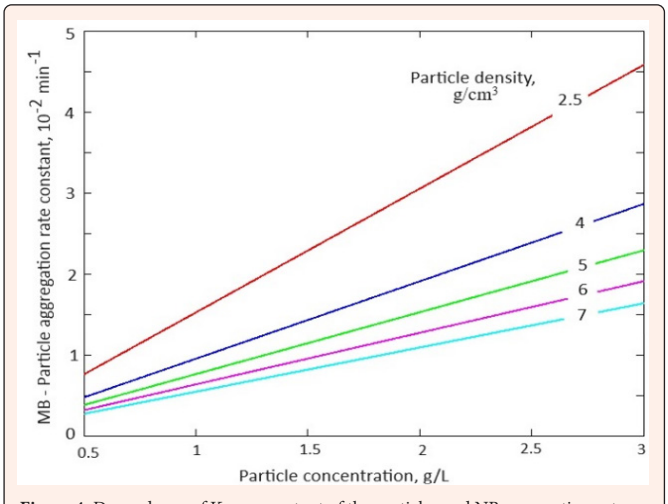

Figure 4: Dependence of $K_{bp\ max}$ constant of the particles and NB aggregation rate on the particles concentration and density: G = 3.6×10^4 min^{-1}; d_b = 0.5 μm; d_p = 10 μm.

Experimental Data

We have to admit that so far, the subject of the combined nano-flotation of ultrafine or fine particles, have not received wide coverage in the academic publications. Most often, NB and MB, were used simultaneously, or actually the mixture of fine and coarse particles was floated. Still, the findings discussed in [26] demonstrate that the application of NB of the size of 0.2 - 0.7 μm increases the recovery of quartz particles of an average size of 8 μm from 75 to 86%. Considering the particle concentration, which was 20 g/l, and applying the formula (8), it is possible to calculate the optimal concentration of NB, which was approximately 4 × 10^{10} NB/mL. The data discussed in [26] have also shown that NB application allows to increase the recovery of quartz particles of an average size of 34 μm from 66 to 84%. In this case, the optimal concentration, calculated by formula (8), was 9 × 10^9 NB/mL. Though this high concentration value of floatable particles occurs rarely, for example, in the scavenging flotation stage, where fine particles take up to 50 wt.%, the obtained results have indicated that NBs have led to the increased the floatability of not just ultrafine, but also fine particles.

The efficiency of combined micro- and nano-flotation of quartz particles of the size of below than 60 μm has been explored in [33]. And the findings have demonstrated that the simultaneous application of NB and MB have improved the recovery of quartz recovery from 72 to 79%. As the MB concentration decreases due to sedimentation, the recovery gradually has fallen to 73%. This result looks quite consistent if we take into account that the particle concentration was 40 g/l, and the NB concentration was 2×10^8 mL^{-1}, which is almost by 3 orders of magnitude below than the optimal value calculated by formula (8).

Conclusion

a. Theoretically, NBs can promote the flotation of fine and ultrafine particles by way of binding them into coarse aggregates.

b. The optimal NB dose depends on NB size, and also on the size and density of the particles and lies in the range (5x10^{-3} - 5x10^{-2}) mL/g.

c. The optimal numerical NB concentration depends on the particle mass concentration, their size and density, and also on the size of NB and is in the range of (10^8-10^9) mL^{-1}.

d. The limiting factors for the practical use of combined nano-flotation are:

   i. Low capacity of conventional methods of NB generation and engineering complexities of producing NB in sufficient quantities directly in the pulp;

   ii. A very low aggregates formation rate in the hydrodynamic field of the flotation call, and for its improvements special units are required which will demand high energy costs and other accompanying expenses.

References

1. Sutherland KL (1948) Physical chemistry of flotation. XI. Kinetics of the flotation process. The Journal of Physical and Colloid Chemistry 52(2): 394-425.

2. Gaudin AM (1957) Flotation (2nd edn), Flotation by Antoine Marc Gaudin, Open Library, McGraw-Hill: New York, US.

3. Tomlinson HS, Fleming MG (1965) Flotation rate studies. Mineral processing: 6th International Congress (Cannes, June 1963): Pergamon Press, London, pp. 562-573.

4. Flint LR, Howarth WJ (1971) Collision efficiency of small particles with spherical air bubbles. Chem Eng Sci 26(8): 1155-1168.

5. Anfruns JF, Kitchener JA (1977) The rate of capture of small particles in flotation. Trans Instit Mining Metall Section C 86: C9.

6. Derjaguin BV, Dukhin SS, Rulev NN (1984) Kinetic theory of flotation of small particles. Surface and Colloid Science; Plenum Press: NY-London, pp. 71-113.

7. Sivamohan R (1990) The problem of recovery of very fine particles in mineral processing - A review. Int J Min Process 28(3-4): 247-288.

8. Forbes E (2011) Shear selective and temperature responsive flocculation: A comparison of fine particle flotation techniques. International Journal of Mineral Processing 99(1-4): 1-10.

9. Yang B, Song S (2014) Hydrophobic agglomeration of mineral fines in aqueous suspensions and its application in flotation: A review. Surface Review and Letters 21(3): 1430003.

10. Read AD, Hollick CT (1976) Selective flocculation techniques for recovery of fine particles. Min Sci Eng 8(3): 202-213.
11. Asgari K, Khoshdast H, Nakhaei F, Garmsiri MR, Huang Q, et al. (2023) Review on floc-flotation of fine particles: technological aspects, mechanisms, and future perspectives. Mineral Processing and Extractive Metallurgy Review.
12. Laskowski JS (1992) An introduction: physicochemical methods of separation. In Colloid Chemistry in Mineral Processing. In: Laskowski JS, Ralston J (Eds.), Amsterdam, The Netherlands: Elsevier 12: 225-241.
13. Huang G, Xu J, Geng P, Li J (2020) Carrier flotation of low-rank coal with polystyrene. Minerals 10(5): 452.
14. Zhou S, Wang X, Bu M, Wang B, An H, et al. (2020) A novel flotation technique combining carrier flotation and cavitation bubbles to enhance separation efficiency of ultra-fine particles. Ultrasonics Sonochemistry 64:105005.
15. Parsonage P (1992) Coating and carrier methods for enhancing magnetic and flotation separations. In Colloid chemistry in mineral processing 12: 361-94.
16. Rodrigues RT, Rubio J (2007) DAF–dissolved air flotation: Potential applications in the mining and mineral processing industry. Int J Miner Process 82(1): 1-13.
17. Yalcin T, Byers A (2006) Dissolved gas flotation in mineral processing. Miner Process Extr Metall Rev 27: 87-97.
18. Rubio J, Carissimi E, Rosa JJ (2007) Flotation in water and wastewater treatment and reuse: recent trends in Brazil. Int J Environment and Pollution 30(2): 193.
19. Rulyov NN, Dontsova TA, Korolyov VY (2007) Separation of fine disperse sorbent from purified water by ultra-flocculation and turbulent micro-flotation. International Journal of Environment and Pollution (IJEP), Special issue: Flotation in Wastewater Treatment, In: Matis KA (Ed.), 30(2): 341-353.
20. Glembotsky VA, Klassen VI (1973) Flotation, Nedra, Moskau.
21. Rulyov NN (2016) Combined microflotation of fine minerals: theory and experiment. Mineral Processing and Extractive Metallurgy (Trans Inst Min Metall C) 125(2): 81-85.
22. Rulyov N 2023) The role of microbubble dose in combined microflotation of fine particles. Preprints.
23. Zhou ZA, Xu Z, Finch JA, Hu H, Rao SR (1997) Role of hydrodynamic cavitation in fine particle flotation. Int J Miner Process 51(1-4): 139-149.
24. Zhou Z, Xu Z, Finch J, Masliyah J, Chow R (2009) On the role of cavitation in particle collection in flotation–A critical review. II. Minerals Engineering 22(5): 419-433.
25. Ahmadi R, Khodadadi DA, Abdollahy M, Fan M (2014) Nano-microbubble flotation of fine and ultrafine chalcopyrite particles. Int J Min Sci Technol 24(4): 559-566.
26. Calgaroto S, Azevedo A, Rubio J (2015) Flotation of quartz particles assisted by nanobubbles. Int J Miner Process 137: 64-70.
27. Azevedo A, Etchepare R, Calgaroto S, Rubio J (2016) Aqueous dispersions of nanobubbles: generation, properties and features. Min Eng 94: 29-37.
28. Tao D, Luttrell G, Yoon RH (2000) A parametric study of froth stability and its effect on column flotation of fine particles. International Journal of Mineral Processing 59(1): 25-43.
29. Tao Y, Liu J, Yu S, Tao D (2006) Picobubble enhanced fine coal flotation. Separation Science and Technology 41(16): 3597-3607.
30. Shi H, Li M, Nikrityuk P, Liu Q (2019) Experimental and numerical study of cavitation flows in venturi tubes: from CFD to an empirical model. Chemical Engineering Science.
31. Oliveira H, Azevedo A, Rubio J (2017) Nanobubbles generation in a high-rate hydrodynamic cavitation tube Minerals Engineering 116: 32-34.
32. Pourkarimi Z, Rezai B, Noaparast M (2017) Effective parameters on generation of nanobubbles by cavitation method for froth flotation application. Physicochem Probl Miner Process 53(2): 920-942.
33. Zhou S, Li Y, Nazari S, Bu X, Hassanzadeh A, et al. (2022) An assessment of the role of combined bulk micro- and nano-bubbles in quartz flotation. Minerals 12(8): 944.
34. Bunkin NF, Shkirin AV (2012) Nanobubble clusters of dissolved gas in aqueous solutions of electrolyte. II. Theoretical interpretation. J Chem Phys 137: 054707.
35. Yurchenko SO, Shkirin AV, Ninham BN, Sychev AA, Babenko VA, et al. (2016) Ion-specific and thermal effects in the stabilization of the gas nanobubble phase in bulk aqueous electrolyte solutions. Langmuir 32(43): 11245-11255.
36. Bunkin NF, Shkirin AV, Suyazov NV, Babenko VA, Sychev AA, et al. (2016) Formation and dynamics of ion-stabilized gas nanobubble phase in the bulk of aqueous NaCl solutions. J Phys Chem B 120(7): 1291-1303.
37. Karakashev SI, Grozev NA (2021) The law of parsimony and the negative charge of the bubbles. Coatings.
38. Gregory J (1988) Polymer adsorption and flocculation in sheared suspensions. Colloids & Surface 31: 231-253.
39. Van de Ven TGM, Masson SG (1977) The microrheology of colloidal dispersions. VII Orthokinetic doublet formation of spheres. Colloid Polym Sci 255: 468-479.
40. Adler PM (1981) Heterocoagulation in shear flow. J Colloid Interface Sci 83(1): 106-115.
41. Rulyov NN, Dontsova TA, Nebesnova TV (2005) The pair binding energy of particles and size flocs, which are formed in the turbulent flow. Khimiya i Tekhnologtya Vody 27: 1-17.